Distributed Formation Control of Non-Holonomic Robots without a Global Reference Frame

Eduardo Montijano, Eric Cristofalo, Mac Schwager and Carlos Sagues

Abstract— **In this paper we consider the problem of controlling a team of non-holonomic robots to reach a desired formation. The formation is described in terms of the desired relative positions and orientations the robots need to keep with respect to each other, and it is assumed that the robots do not have a common shared reference frame. In other words, the robots can use only on-board sensing to achieve the formation. We first consider a holonomic framework, using a well known distance-based approach to reach a formation for the positions. We then include a control law for the orientations. We further discuss the problem of mirror configurations that appear when different desired relative orientations can satisfy the same distance-based constraints through different formations. Exploiting the concept of chirality, we present a relabelling strategy to reassign the robots' roles to reach the desired pattern when a mirror configuration occurs. The distance-based holonomic control is then transformed to cope with the non-holonomic constraints using a piecewise-smooth function. Simulation results, as well as hardware experiments with five m3pi robots demonstrate the applicability of our approach.**

I. Introduction

Teams of robots acting cooperatively can be useful in a broad array of applications, including multi-robot manipulation [1], entertainment [2], or search and rescue missions [3]. One of the first challenges that any successful multi-robot system needs to face is the coordinated motion of all of its members, reaching a desired configuration to accomplish a task.

For this reason formation control is one of the most widely studied problems in multi-robot systems [4]. Exploiting the information only from nearest neighbors [5], the whole team can reach many different configurations without the need of a global coordinator. Some approaches are based on inter robot positions [6], bearings [7] and distances [8], [9], whereas the influence of different orientations in the relative positions has been discussed in [10], [11]. However, in these solutions the robots are modeled as single integrators. Since the control is designed by decoupling the rotations from the translation, these techniques are not readily applied to robots with non-holonomic motion constraints.

E. Montijano is with Centro Universitario de la Defensa (CUD) and Instituto de Investigación en Ingeniería de Aragón (I3A), Zaragoza, Spain. emonti@unizar.es

E. Cristofalo is with Department of Mechanical Engineering, Boston University, Boston, USA. emc73@bu.edu

M. Schwager is with Department of Aeronautics and Astronautics, Stanford University, Stanfod, USA. schwager@stanford.edu

C. Sagues is with Departamento de Informática e Ingeniería de Sistemas - Instituto de Investigación en Ingeniería de Aragón (I3A), Universidad de Zaragoza, Spain. csagues@unizar.es

This work was supported by Spanish projects TELOMAN (DPI2012-32100), SIRENA (CUD2013-05) and grant CAS14/00205, and in part by NSF grants CNS-1330008 and IIS-1350904. We are grateful for this support.

Since unicycle robots are widely popular commercial platforms, the formation control problem for these robots has also been analyzed in the literature. Nearest neighbor approaches have been successfully used for flocking [12] and rendez-vous [13], [14]. Unfortunately, when the goal is to reach relative positions, most of the available solutions rely on leader-follower scenarios [15], [16], where each robot controls its motion using only the information of another single robot, its leader in the formation, or individual reference trajectories [17]–[19] independent of other robots' motion. Full formation using information from multiple neighbors is discussed in [20] and [21], but to reach the formation it is required for all the robots to share a global reference frame.

In this paper we present a formation control strategy for non-holonomic robots that uses nearest-neighbors rules without a global frame and considering different final orientations. We describe the formation objective by means of the relative positions and orientations the robots need to keep with respect to each other. Firstly, we consider a holonomic version of the problem, combining a distance based controller for the positions with an angular velocity that does not depend on the orientations of the other robots. This way, the orientation of each robot can be used as a degree of freedom to reach the desired formation in the non-holonomic case. In a second stage the non-holonomic inputs are defined using a smooth piecewise function of the holonomic ones. In the paper we also analyze the implications that relative positions and orientations have in a purely distance-based solution. In particular, we characterize the impossibility of reaching the desired configuration in the case of reflections of the formation without further actions. For the specific set of achiral formations, we propose a relabelling strategy of the roles of the robots such that, in the case of a reflection, the team still reaches the desired configuration without the need of further motion. The whole approach is validated by means of simulations and with real experiments.

The rest of the paper is arranged as follows. Section II introduces some necessary notation and concepts and gives a formal description of the formation control problem. A distance-based holonomic solution, including different final desired orientations is presented in Section III. The transformation of the holonomic solution to non-holonomic motion constraints is described in Section IV. Section V includes some simulation results and experiments with real robots are reported in Section VI. Finally, the conclusions of this work are in Section VII.

II. Notation and Problem Setup

A. Robots and coordinate systems

Let us consider a team of N robots. The position and orientation of robot i in the world coordinate frame are denoted by $\mathbf{p}_i = [x_i, y_i]^T$ and θ_i respectively. The motion of the robots is governed by non-holonomic unicycle dynamics,

$$\begin{bmatrix} \dot{x}_i \\ \dot{z}_i \\ \dot{\theta}_i \end{bmatrix} = \begin{bmatrix} \cos(\theta_i) & 0 \\ \sin(\theta_i) & 0 \\ 0 & 1 \end{bmatrix} \begin{bmatrix} v_i \\ w_i \end{bmatrix}, \tag{1}$$

where v_i and w_i are the robot's linear and angular velocities. The rotation matrix associated to θ_i is denoted by $\mathbf{R}_i$,

$$\mathbf{R}(\theta_i) \equiv \mathbf{R}_i = \begin{pmatrix} \cos(\theta_i) & -\sin(\theta_i) \\ \sin(\theta_i) & \cos(\theta_i) \end{pmatrix}. \tag{2}$$

Given two robots, we denote by $\mathbf{p}_{ij}$ the relative position of robot j locally measured by robot i,

$$\mathbf{p}_{ij} = [x_{ij}, y_{ij}]^T = \mathbf{R}_i^T(\mathbf{p}_j - \mathbf{p}_i), \tag{3}$$

whereas the relative orientation, θ_{ij}, is determined by the angle described by the rotation matrix

$$\mathbf{R}_{ij} = \mathbf{R}_i^T \mathbf{R}_j. \tag{4}$$

With a slightly abuse of notation, we denote $\theta(\mathbf{R}) \in (-\pi, \pi]$ the operator to compute the angle from the roation matrix, considering always the smallest geodesic distance in the rotation matrix. Note that $\theta(\mathbf{R})$ is the inverse operation of (2) and that both operations work independently of the coordinate system, i.e., they can be used in any frame. Therefore, $\theta_{ij} = \theta(\mathbf{R}_{ij})$, which might not necessarily be equal to $\theta_j - \theta_i$. Additionally, we denote by d_{ij} the relative distance between the robots

$$d_{ij} = \|\mathbf{p}_{ij}\|. \tag{5}$$

All these elements are illustrated in Fig. 1.

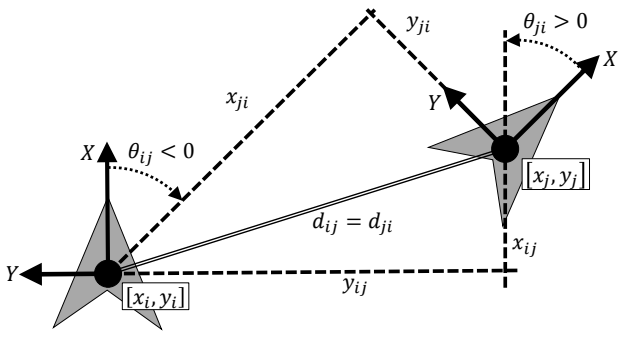

Fig. 1. Relative positions and orientations of two robots.

The sensing between pairs of robots is limited to a subset of the whole team. This limitation is encoded in the interaction graph $\mathcal{G} = (\mathcal{V}, \mathcal{E})$. The nodes in the graph, $\mathcal{V}$, represent the different robots of the team, whereas the edges, $(i, j) \in \mathcal{E}$, represent the availability of the relative position and orientation of robot j, $[\mathbf{p}_{ij}, \theta_{ij}]$, to robot i. This way, the set of robots observed by robot i is denoted by $\mathcal{N}_i$.

B. Formation definition

The formation control problem is defined by a set of desired relative positions and orientations between different pairs of robots, $\mathbf{p}_{ij}^*$ and θ_{ij}^*. We impose an assumption on the feasibility of such formation.

***Assumption** 2.1: (Feasible configuration).* The desired configuration can be achieved by the team, in the sense that all the relative positions and orientations are consistent with each other. Formally speaking, it must hold that

$$\mathbf{p}_{ij}^* = \mathbf{p}_{ik}^* + \mathbf{R}_{ik}^* \mathbf{p}_{kj}^*, \tag{6}$$

and $\mathbf{R}_{ij}^* = \mathbf{R}_{ik}^* \mathbf{R}_{kj}^*$ for all $i, j, k \in \mathcal{V}$.
Note that there are infinite sets of positions for the robots such that they satisfy (6), all of them related by some rotation and translation. Also note that in general $\mathbf{p}_{ij} \neq -\mathbf{p}_{ji}$.

C. Geometry definitions

Given a vector, $\mathbf{v} = [v_x, v_y]^T$, we denote

$$\mathbf{R}(\mathbf{v}) = \frac{1}{\|\mathbf{v}\|} \begin{pmatrix} v_x & -v_y \\ v_y & v_x \end{pmatrix} \tag{7}$$

the rotation matrix that describes that vector.

***Definition** 2.2 (Mirror operation):* Given a line $\ell \equiv \mathbf{p} + \lambda \mathbf{v}$, $\mathbf{p}, \mathbf{v} \in \mathbb{R}^2, \lambda \in \mathbb{R}$, the mirror operation, $\mathcal{M}(\mathbf{p}_i, \ell)$, of the point $\mathbf{p}_i$ in ℓ is defined as the operation of computing the refection of $\mathbf{p}_i$ with respect to ℓ. This operation can be computed using the following product

$$\mathcal{M}(\mathbf{p}_i, \ell) = \mathbf{R}(\mathbf{v}) \mathbf{R}_{\mathcal{M}} \mathbf{R}(\mathbf{v})^T (\mathbf{p}_i - \mathbf{p}) + \mathbf{p} \tag{8}$$

with $\mathbf{R}(\mathbf{v})$ given in (7) and

$$\mathbf{R}_{\mathcal{M}} = \begin{pmatrix} 1 & 0 \\ 0 & -1 \end{pmatrix}. \tag{9}$$

The mirror operation is an isometry in any set of points, i.e., its application to a set of points preserves the distances between all of them. Also note that the matrix $\mathbf{R}_{\mathcal{M}}$ is a 3D rotation matrix of π radians along a parallel axis to the plane of motion (in this case the x-axis), which consequently cannot be put in the form (2).

Although the whole setup is defined in terms of relative information, for the theoretical analysis and upcoming explanations, it is convenient to consider the positions and orientations measured in the world frame. Denote by $\mathbf{p}_i^*$ and θ_i^* a set of positions and orientations such that, using (2)-(4), satisfies Assumption 2.1.

The next definition categorizes all the possible formations in terms of the mirror operation.

***Definition** 2.3 (Achiral formation):* The set of positions that configure a formation is defined *achiral* if, for every $\mathbf{p}_i^*$ and any line ℓ, there exists another position in the formation, $\mathbf{p}_j^*$, a translation, $\mathbf{t}_\mathbf{m}$, and a rotation, $\mathbf{R}_\mathbf{m}$, such that

$$\mathbf{p}_j^* = \mathbf{R}_\mathbf{m} \mathcal{M}(\mathbf{p}_i^*, \ell) + \mathbf{t}_\mathbf{m}. \tag{10}$$

Otherwise the positions in the formation are defined to be *chiral*.

These concepts are all shown in Fig. 2.

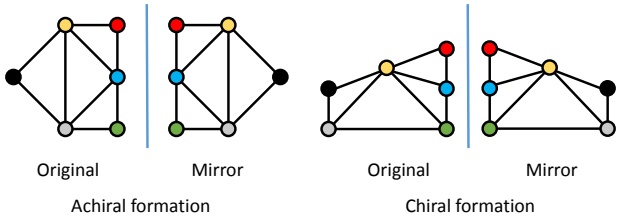

Fig. 2. Two examples of set of positions and their corresponding mirror configurations. The left configuration is achiral because the original pattern can be recovered from the mirror by a translation, a rotation and a relabeling of the points. The right formation is chiral because the same type of recovery is not possible.

III. Holonomic Control

Before considering the non holonomic motion of the robots, we start discussing a simplified holonomic version of the setup that will serve as the base for the general case. Let us denote $\mathbf{u}_i$ the kinematic velocity of robot i, expressed in its own frame. The evolution of the position of the holonomic robot in the world frame is then $\dot{\mathbf{p}}_i = \mathbf{R}_i \mathbf{u}_i$.

We adopt a distance-based formulation to design $\mathbf{u}_i$. In particular, following existing literature [8], [9], each robot computes its kinematic velocity by

$$\mathbf{u}_i = K_u \sum_{j \in \mathcal{N}_i} \left(d_{ij} - d^*_{ij}\right) \frac{\mathbf{p}_{ij}}{\|\mathbf{p}_{ij}\|}, \tag{11}$$

with K_u some positive gain. Note that only relative information is considered in the computation of (11).

The main reason for adopting this controller, instead of a solution such as [10], is that the motion of the robots is not affected by their orientation. For any value of $\mathbf{R}_i$, the transformation of $\mathbf{u}_i$ to the world coordinate frame is always the same

$$\mathbf{u}_{wi} = \mathbf{R}_i \mathbf{u}_i = K_u \sum_{j \in \mathcal{N}_i} \left(d_{ij} - d^*_{ij}\right) \left(\mathbf{p}_j - \mathbf{p}_i\right). \tag{12}$$

This degree of freedom will be exploited in the next section to develop the non-holonomic controller.

Since existing literature already provides a convergence analysis using this controller [8], [9], we do not enter much into details. If the interaction graph $\mathcal{G}$ with respect to the desired positions describes a rigid figure, then (11) is locally asymptotically stable. In addition, the final configuration is the desired one up to a congruence (translation, rotation and, possibly, a mirror operation), i.e.,

$$\mathbf{p}_i = \mathbf{R}^* \mathbf{p}^*_i + \mathbf{t}^* \tag{13}$$

or

$$\mathbf{p}_i = \mathbf{R}^* \mathcal{M}(\mathbf{p}^*_i, \ell^*) + \mathbf{t}^*, \tag{14}$$

with $\mathbf{R}^*$, $\mathbf{t}^*$ and ℓ^* some rotation, translation and line respectively. From now on, we assume that the conditions for convergence to either of these configurations are met and we discuss how to design the angular velocity and the implications of reaching (13) or (14).

In order to reach the desired relative orientations, we propose to use to following control law,

$$w_i = K_w \sum_{j \in \mathcal{N}_i} \theta\Big(\mathbf{R}(\mathbf{p}^*_{ij})^T \mathbf{R}(\mathbf{p}_{ij})\Big). \tag{15}$$

In the above equation (7) has been used to compute the rotation matrices, and the operator $\theta(\cdot)$ is used to compute the associated angle. From a geometrical point of view, the term $\theta(\mathbf{R}(\mathbf{p}^*_{ij})^T \mathbf{R}(\mathbf{p}_{ij}))$ represents the angle from $\mathbf{p}^*_{ij}$ to $\mathbf{p}_{ij}$, see Fig. 3. Note that in (15), w_i does not depend on the orientations of other robots, θ_j.

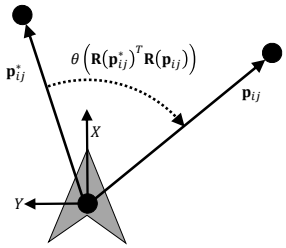

Fig. 3. Design of the angular velocity.

Let us start analyzing the behavior of the orientations under the assumption of fixed desired positions, i.e., $\mathbf{u}_i = \mathbf{0}$ for all i and either (13) or (14) hold.

***Proposition** 3.1 (Convergence for* (13)*):* Assume that the desired formation satisfies Assumption 2.1 and the positions of the robots are fixed and equal to (13). Then, for any initial orientations, using the angular velocity in (15) the orientations of all the robots converge to fixed values θ^*_i such that $\mathbf{R}_{ij} = \mathbf{R}^*_{ij}$ for all $i, j \in \mathcal{V}$.

Proof: First of all, since the angular velocities of the robots do not depend on the orientation of any robot but themselves, we can analyze the behavior of θ_i individually, without consider other robots rather than i.

The first thing we demonstrate is the existence of a fixed point, θ^*_i. The existence of such point necessarily implies that, if $\theta_i = \theta^*_i$, then $w_i = 0$. Consider some $j \in \mathcal{N}_i$. Using (13), the term in w_i associated to such robot is

$$\begin{aligned} &\theta\Big(\mathbf{R}(\mathbf{p}^*_{ij})^T \mathbf{R}(\mathbf{p}_{ij})\Big) = \\ &\quad \theta\Big(\mathbf{R}(\mathbf{p}^*_j - \mathbf{p}^*_i)^T \mathbf{R}^*_i \mathbf{R}^T_i \mathbf{R}^* \mathbf{R}(\mathbf{p}^*_j - \mathbf{p}^*_i)\Big) = \\ &\quad \theta\Big(\mathbf{R}^*_i \mathbf{R}^T_i \mathbf{R}^* \mathbf{R}(\mathbf{p}^*_j - \mathbf{p}^*_i)^T \mathbf{R}(\mathbf{p}^*_j - \mathbf{p}^*_i)\Big) = \\ &\quad \theta\Big(\mathbf{R}^*_i \mathbf{R}^T_i \mathbf{R}^*\Big), \end{aligned} \tag{16}$$

where the fact that the product of matrices is commutative in $SO(2)$ has been used in the second equality.

Therefore, all the neighbors generate the same amount of angular input in w_i and

$$w_i = 0 \Longleftrightarrow \mathbf{R}_i = \mathbf{R}^* \mathbf{R}^*_i. \tag{17}$$

Thus, there exists a fixed point, $\theta^*_i = \theta\Big(\mathbf{R}^* \mathbf{R}^*_i\Big)$, which is also unique.

The next step is to show that the angular position of the robot converges to such point using (15). Consider the following candidate Lyapunov function

$$V = \frac{1}{2}\theta\left(\mathbf{R}(\theta_i^*)^T\mathbf{R}(\theta_i)\right)^2 > 0. \tag{18}$$

After some algebraic calculations, the derivative of the Lyapunov function is given by

$$\dot{V} = \theta\left(\mathbf{R}(\theta_i^*)^T\mathbf{R}(\theta_i)\right)w_i. \tag{19}$$

Let us start considering the case where $\theta\left(\mathbf{R}(\theta_i^*)^T\mathbf{R}(\theta_i)\right) < 0$. Replacing the value of θ_i^*

$$\theta\left(\mathbf{R}(\theta_i^*)^T\mathbf{R}(\theta_i)\right) = \theta\Big((\mathbf{R}_i^*)^T(\mathbf{R}^*)^T\mathbf{R}_i\Big) = -\theta\Big(\mathbf{R}_i^*\mathbf{R}_i^T\mathbf{R}^*\Big). \tag{20}$$

Therefore, in this case $\dot{V} < 0$. The case where $\theta\left(\mathbf{R}(\theta_i^*)^T\mathbf{R}(\theta_i)\right) > 0$ can be made analogously, demonstrating that the orientation of the robot converges to θ_i^*.

Finally, knowing that $\mathbf{R}_i \to \mathbf{R}^*\mathbf{R}_i^*$ for all i, we reach that $\mathbf{R}_{ij} \to \mathbf{R}_{ij}^*$ for all i and j and the whole desired formation is achieved. ∎

In order to show that the angular controller can be used simultaneously to the position controller, we would need to consider $\theta\Big(\mathbf{R}(\mathbf{p}_{ij}^*)^T\mathbf{R}(\mathbf{p}_{ij})\Big)$ as a perturbed version of the one analyzed in the previous proposition, with the perturbation asymptotically going to zero due to the convergence of (11). Nevertheless, since our goal is to exploit the degree of freedom of the rotation to derive the non-holonomic controller, we leave this demonstration for future work.

The next issue to consider is to see what happens when the positions of the robots converge to (14). Unfortunately, in this case, noting that $\mathbf{R}(\mathbf{R}_{\mathcal{M}}\mathbf{p}) = \mathbf{R}(\mathbf{p})^T$, the terms in the angular velocity for each neighbor are not equal,

$$\begin{aligned}&\theta\Big(\mathbf{R}(\mathbf{p}_{ij}^*)^T\mathbf{R}(\mathbf{p}_{ij})\Big) = \\ &\theta\Big(\mathbf{R}_i^*\mathbf{R}_i^T\mathbf{R}^*\mathbf{R}(\mathbf{v}^*)\mathbf{R}(\mathbf{v}^*)\mathbf{R}(\mathbf{p}_j^* - \mathbf{p}_i^*)^T\mathbf{R}(\mathbf{p}_j^* - \mathbf{p}_i^*)^T\Big),\end{aligned} \tag{21}$$

with $\mathbf{R}(\mathbf{v}^*)$ the vector associated to ℓ^* as in (7). While convergence to a fixed point can still be proved, the new closed loop system might have more than one of these stationary points, and none of them will be able to satisfy that $\mathbf{R}_{ij} = \mathbf{R}_{ij}^*$ for all i and j in the team. This implies that, whenever a reflection of the formation occurs, even when the distances between robots are the desired ones, the relative positions and orientations will not reach the desired formation using (11) and (15).

Nevertheless, for the set of achiral formations, the robots can apply a simple relabeling of their roles that will allow them reach the desired configuration. If a formation is achiral, then it means that it has at least one line of symmetry (it can have more), which we denote by ℓ_S. Under this reflection, the rotation and translation in (10) are $\mathbf{R_m} = \mathbf{I}$ and $\mathbf{t}_m = \mathbf{0}$. Thus, for all i, there exists another robot j such that

$$\mathbf{p}_j^* = \mathcal{M}(\mathbf{p}_i^*, \ell_S) = \mathbf{R}(\mathbf{v}_S)\mathbf{R}_{\mathcal{M}}\mathbf{R}(\mathbf{v}_S)^T(\mathbf{p}_i^* - \mathbf{p}_S) + \mathbf{p}_S. \tag{22}$$

Thus, if each robot assumes the role of its reflected comrade, denoted for brevity $\mathcal{M}_i$, eq. (21) becomes

$$\begin{aligned}&\theta\Big(\mathbf{R}(\mathbf{p}_{\mathcal{M}_i\mathcal{M}_j}^*)^T\mathbf{R}(\mathbf{p}_{ij})\Big) = \\ &\theta\Big(\mathbf{R}_{\mathcal{M}_i}^*\mathbf{R}_i^T\mathbf{R}^*\mathbf{R}(\mathbf{v}^*)\mathbf{R}(\mathbf{v}^*)\mathbf{R}(\mathbf{v}_S)^T\mathbf{R}(\mathbf{v}_S)^T\Big),\end{aligned} \tag{23}$$

and the analysis in Proposition 3.1 can be reused to show that $\mathbf{R}_{ij} \to \mathbf{R}_{\mathcal{M}_i\mathcal{M}_j}^*$. This, combined with (14), shows that the whole team reaches again the desired pattern with different roles.

***Remark** 3.2 (Reflection detectability):* Note that the robots can detect individually whether they are converging to the original desired pattern or the mirror one simply by checking if the different terms $\theta\Big(\mathbf{R}(\mathbf{p}_{ij}^*)^T\mathbf{R}(\mathbf{p}_{ij})\Big)$ are equal to zero at the equilibrium or not.

IV. Non Holonomic Control

In this section we focus on applying the distance based controller (11) to non-holonomic robots. First of all, with the objective of abbreviate the notation, let $\beta_{ij} = \mathbf{R}(\mathbf{p}_{ij})$ be the bearing angle of robot j with respect to robot i. Additionally, let ρ_i and ϕ_i be the polar coordinates of the holonomic input $\mathbf{u}_i$ with respect to robot i frame, i.e.,

$$\rho_i = \|\mathbf{u}_i\| \text{ and } \phi_i = \theta(\mathbf{R}(\mathbf{u}_i)). \tag{24}$$

The open loop relative motion of robot j in the frame of robot i is given by

$$\dot{d_{ij}} = -v_i\cos\beta_{ij} - v_j\cos\beta_{ji}, \tag{25}$$

and

$$\dot{\beta_{ij}} = v_i\frac{\sin\beta_{ij}}{d_{ij}} + v_j\frac{\sin\beta_{ji}}{d_{ij}} - w_i. \tag{26}$$

Using these two expressions, we can compute the open loop evolution of the holonomic input $\mathbf{u}_i$ in (11),

$$\begin{aligned}\dot{u}_i^x =& -|\mathcal{N}_i|v_i + \sum_{j\in\mathcal{N}_i}(v_j\cos\theta_{ji}) + u_i^y w_i + \\ &\sum_{j\in\mathcal{N}_i}\left(\frac{d_{ij}^*}{d_{ij}}\sin\beta_{ij}\left(v_i\sin\beta_{ij} + v_j\sin\beta_{ji}\right)\right),\end{aligned} \tag{27}$$

$$\begin{aligned}\dot{u}_i^y =& -\sum_{j\in\mathcal{N}_i}(v_j\sin\theta_{ji}) - u_i^x w_i - \\ &\sum_{j\in\mathcal{N}_i}\left(\frac{d_{ij}^*}{d_{ij}}\cos\beta_{ij}(v_i\sin\beta_{ij} + v_j\sin\beta_{ji})\right).\end{aligned} \tag{28}$$

Similarly, the open loop evolution in polar coordinates is

$$\begin{aligned}\dot{\rho}_i =& -|\mathcal{N}_i|v_i\cos\phi_i + \sum_{j\in\mathcal{N}_i}v_j\cos(\phi_i - \theta_{ij}) \\ &+ \sum_{j\in\mathcal{N}_i}\left(\frac{d_{ij}^*}{d_{ij}}\sin(\beta_{ij} - \phi_i)(v_i\sin\beta_{ij} + v_j\sin\beta_{ji})\right)\end{aligned} \tag{29}$$

$$\begin{aligned}\dot{\phi}_i =& -w_i + \frac{|\mathcal{N}_i|v_i\sin\phi_i}{\rho_i} - \sum_{j\in\mathcal{N}_i}\frac{v_j\sin(\phi_i - \theta_{ji})}{\rho_i}, \\ &+ \sum_{j\in\mathcal{N}_i}\left(\frac{d_{ij}^*}{d_{ij}}\frac{\cos(\beta_{ij} + \phi_i)}{\rho_i}\left(v_i\sin\beta_{ij} + v_j\sin\beta_{ji}\right)\right).\end{aligned} \tag{30}$$

Given some relative goal, as is $\mathbf{u}_i$, a typical approach to control a non-holonomic vehicle consists in letting $v_i = \rho_i$ and $w_i = \phi_i$. If the goal is fixed, this simple control law drives the robot towards it, no matter where it is [18]. However, in our case, the evolution of the goal along with the highly coupling with the neighbors' positions implies that this solution won't always work. We propose instead a similar control design, piecewise defined depending on the holonomic inputs.

In particular, the linear velocity of each robot is designed according to the following rule:

$$v_i = \begin{cases} \rho_i & \text{if } \frac{-\pi}{4} < \phi_i \leq \frac{\pi}{4} \\ \frac{\rho_i}{\tan(\phi_i)} & \text{if } \frac{\pi}{4} < \phi_i \leq \frac{3\pi}{4} \\ \frac{-\rho_i}{\tan(\phi_i)} & \text{if } \frac{-3\pi}{4} < \phi_i \leq \frac{-\pi}{4} \\ -\rho_i & \text{otherwise} \end{cases}, \tag{31}$$

whereas the angular velocity is defined by

$$w_i = \begin{cases} \phi_i & \text{if } \frac{-\pi}{2} < \phi_i \leq \frac{\pi}{2} \\ \phi_i + \pi & \text{otherwise} \end{cases}. \tag{32}$$

For a better understanding of the controller, these two equations are graphically shown in Fig. 4.

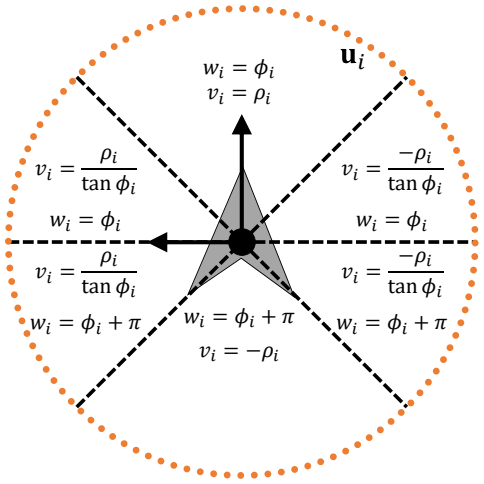

Fig. 4. Non holonomic inputs as a function of $\mathbf{u}_i$.

The complexity of the closed-loop equations resulting of the combination of (31) and (32) with either (27)-(28) or (29)-(30) makes it hard to provide a formal demonstration of convergence of the whole system. Nevertheless, in the following we provide the intuition behind the control inputs and we show in simulations and experiments with real robots that our solution performs well enough to be applicable.

The control input (31) is designed to move always in the direction that reduces the value of ρ_i (forward or backward). The tangents make smooth the transition between moving forward and moving backward, avoiding the discontinuity that happens when the goal is perpendicular to the direction of the robot. This way, we can avoid shaky motions of the robots.

The angular velocity in Eq. (32) is designed to steer the robot in such a way that it is aligned with the goal in the shortest angular path (clockwise or anticlockwise). This way, the robots behave much closer to how they would if they were holonomic. In this case there is a discontinuity when $\phi_i = \pm\pi/2$. However, the angular velocities at both sides of the discontinuities drive the value of ϕ_i away from these points. If we combine this with the fact that at those values of ϕ_i the linear velocity is zero, we reach that once again shaky motions of the robots are avoided.

Note that these inputs drive the robots towards the positions that satisfy the desired relative distances between each other but do not account for the final desired relative orientations. Whenever the robots detect that they are sufficiently close to the desired distance values, they locally change the angular rates computed in (32) for those given in Eq. (15).

V. Simulations

Some simulations have been run in Matlab to test our proposal. A comparison of different holonomic and non-holonomic solutions is provided in Fig. 5 for a team of 6 robots. In the top left plot of Fig. 5 we show the desired formation pattern (a regular hexagon), with blue lines denoting neighbors in the communication graph. The formation is infinitesimally rigid, and thus we can guarantee local stability of the distance-based holonomic formation control. The initial position of the robots for all the controllers is shown in the top right plot of Fig. 5.

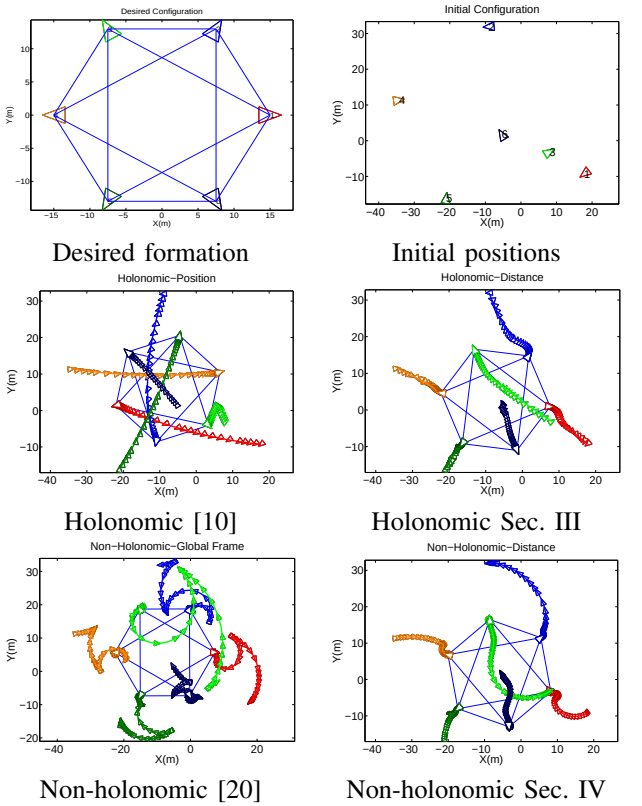

Fig. 5. Comparison of different formation control strategies.

The middle plots show the trajectories using two holonomic controllers. The consensus-based formation control using relative positions proposed in [10] is shown in the left

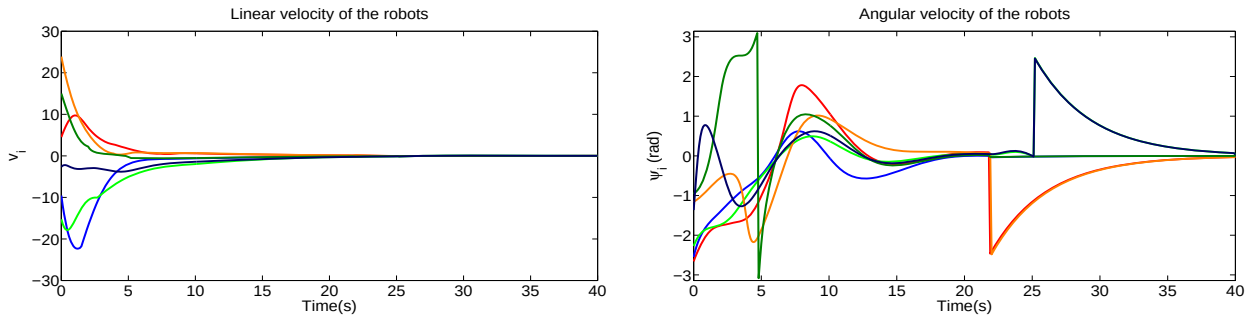

(a) Linear velocities (b) Angular velocities

Fig. 6. Velocities for the non-holonomic trajectory in Fig. 5 (e).

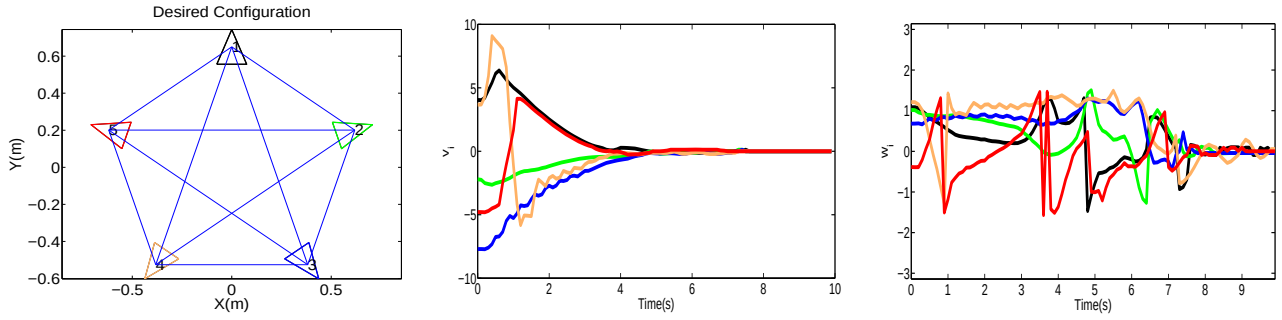

(a) Desired formation (b) Linear velocities (c) Angular velocities

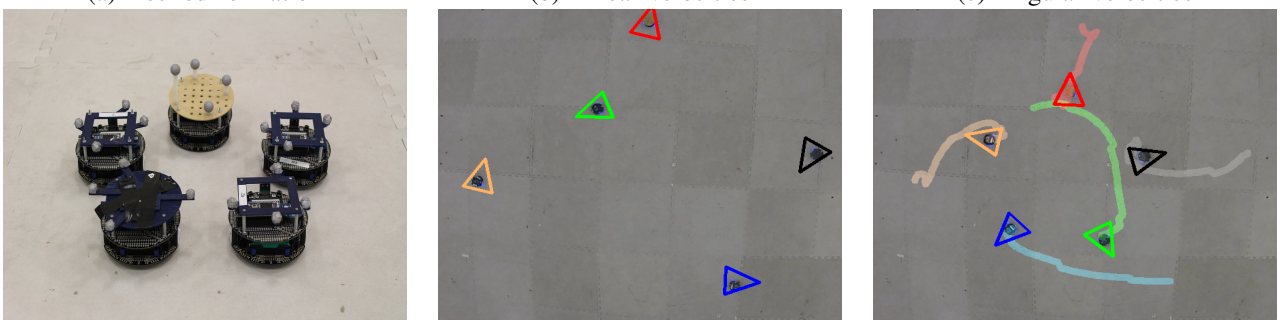

(d) M3Pi robots (e) Initial Positions (f) Final configuration

Fig. 7. Non-holonomic formation control with real robots.

plot and the distance-based holonomic control with different orientations, Eqs. (11) and (15), given in Section III is shown on the right. In this case the robots converge to the right configuration, so no relabelling is required. By using inter-robot distances, the path travelled by the robots is smaller than that of [10].

The bottom plots of Fig. 5 show the trajectories using two non-holonomic solutions. On the left we can see the trajectories using the solution presented in [20], where the robots require some common reference frame to reach the formation. The solution we have proposed in Section IV is shown on the bottom right plot, which makes the robots travel less distance and also does not require a global frame. The trajectory is slightly longer to that of the equivalent holonomic approach, but it accounts for the real dynamics of most ground robots.

The linear and angular velocities of the proposed non-holonomic solution are depicted in Fig. 6. The linear velocity of the robots is shown on the left graphic and the angular velocity on the right one. As mentioned in the paper, we can observe how the linear velocities follow smooth trajectories, even under abrupt changes in the angular velocities, for example at time $t = 5s$ for the dark green robot. The angular velocities are also in general quite smooth. The transition between the angular velocities in (32) used to reach the desired distances and the angular velocities in (15) to reach the desired relative orientations can be clearly observed for the dark blue, red and orange robots at times $t = 22s$ and $t = 25s$. The threshold to switch from one velocity to the other has been set at $5cm$.

VI. Experiments

We have also conducted real experiments with 5 m3pi robots to validate our controller (Fig. 7 (d)). Since how the robots perceive their neighbors is outside of the scope of this paper, we have used the Optitrack system to compute the relative position and orientation between the robots. Using these relative positions, the control commands are

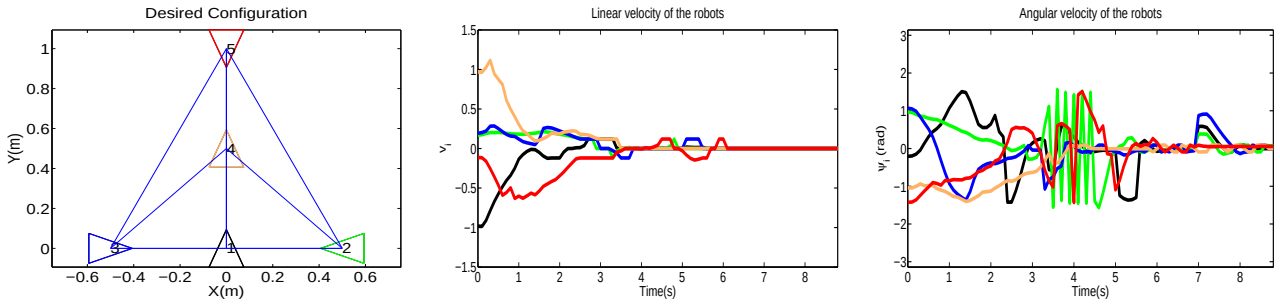

(a) Desired formation (b) Linear velocities (c) Angular velocities

(d) Initial Positions (e) Convergence to (14) (f) Formation after relabelling

Fig. 8. Real experiment with convergence to a mirror configuration (14) and correction using the relabelling in (22).

computed in Matlab and sent to each of the robots via XBee devices at 10Hz. In the paper we present two different formation experiments. Additional formations can be seen in the supplementary video.

The desired formation of the first experiment has been defined as a regular polygon with the orientation of each robot pointing outwards, as shown in Fig. 7 (a). The initial configuration of the robots is shown in Fig. 7 (e). For a better visualization we have overimposed in the image the Optitrack measurements of each robot. The trajectories and final configuration are shown in Fig. 7 (f), where we can see that the whole team reaches the desired formation. The linear velocities, computed using (31) are shown in Fig. 7 (b), whereas the angular ones, using (32) and (15) when the distances are near zero (approximately at time $t = 5s$), are depicted in Fig. 7 (c).

In Figure 8 we show another formation experiment in which the team converges to a mirror configuration. Figure 8 (a) shows the desired configuration with a T shape and Fig. 8 (d) the initial configuration. After running the controller, the team reaches the configuration in Fig. 8 (e) where it can be seen that the inter-robot distances are preserved but robots 2 (blue) and 3 (green) are mirrored. Each robot individually detects this situation and execute the prespecified relabelling which changes the role of robots 2 and 3. This change can be observed in Fig. 8 (c) at time 7, where there is a spike on the angular velocity of several robots. The final configuration is shown in Fig. 8 (f) where the pattern with the change of roles is correct.

VII. Conclusions

In this paper we have analyzed the formation control problem with a team of non-holonomic robots without global information. Both the formation and the control design are defined by means of the relative positions and orientations of the robots with respect to each other. We have started considering holonomic robots, combining a distance-based position control with a new angular velocity design, showing convergence to the desired configuration. In the case of achiral formations, the possible convergence to a mirror pattern has been overcome by a role change of the robots. In a second stage, we have exploited the independence of the robot orientations in the holonomic case to present a non-holonomic control strategy to reach the desired formation. Simulation results and experiments with real robots have been used to show the behavior of our proposed control strategy.

References

[1] Z. Wang and M. Schwager. Multi-robot manipulation without communication. In *International Symposium on Distributed Autonomous Robotic Systems*, 2014.

[2] J. Alonso-Mora, A. Breitenmoser, M. Rufli, R. Siegwart, and P. Beardsley. Image and animation display with multiple mobile robots. *The International Journal of Robotics Research*, 31(6):753–773, June 2012.

[3] D. Tardioli, D. Sicignano, L. Riazuelo, A. Romeo, J. L. Villarroel, and L. Montano. Robot teams for intervention in confined and structured environments. *Journal of Field Robotics*, 2015.

[4] K-K. Oh, M-C Park, and H-S. Ahn. A survey of multi-agent formation control. *Automatica*, 53(3):424–440, March 2015.

[5] A. Jadbabaie, J. Lin, and A.S. Morse. Coordination of Groups of Mobile Autonomous Agents using Nearest Neighbor Rules. *IEEE Transactions on Automatic Control*, 48(6):988–1001, June 2003.

[6] J. Cortés. Global and robust formation-shape stabilization of relative sensing networks. *Automatica*, 45(12):2754–2762, Dec 2009.

[7] A. Franchi, C. Masone, V. Grabe, M. Ryll, H. H. Bulfhoff, and P. R. Giordano. Modeling and control of UAV bearing formations with bilateral high-level steering. *International Journal of Robotics Research*, 31:1504–1525, Dec 2012.

[8] L. Krick, M. E. Broucke, and B. A. Francis. Stabilization of infinitesimally rigid formations of multi-robot networks. In *IEEE International Conference on Decision and Control*, pages 477–482, Dec 2008.

[9] K-K Oh and H-S Ahn. Formation control of mobile agents based on inter-agent distance dynamics. *Automatica*, 47(10):2306–2312, Oct 2011.

[10] E. Montijano, D. Zhou, M. Schwager, and C. Sagues. Distributed formation control without a global reference frame. In *American Control Conference*, pages 3862–3867, June 2014.

[11] K-K. Oh and H-S. Ahn. Formation control and network localization via orientation alignment. *IEEE Transactions on Automatic Control*, 59(2):540–545, February 2014.

[12] E. Montijano, J. Thunberg, X. Hu, and C. Sagues. Epipolar visual servoing for multi-robot distributed consensus. *IEEE Transactions on Robotics*, 29(5):1212–1225, Oct 2013.

[13] D. V. Dimarogonas and K. J. Kyriakopoulos. On the rendezvous problem for multiple nonholonomic agents. *IEEE Transactions on Automatic Control*, 52(5):916–922, May 2007.

[14] K.D. Listmann, M. V. Masalawala, and J. Adamy. Consensus for formation control of nonholonomic mobile robots. In *IEEE International Conference on Robotics and Automation*, pages 3886–3891, May 2009.

[15] A. Das, R. Fierro, V. Kumar, J. Ostrowski, J. Spletzer, and C. J. Taylor. Vision based formation control of multiple robots. *IEEE Transactions on Robotics and Automation*, 18(5):813–825, Oct 2002.

[16] T. Gustavi and X. Hu. Observer-based leader-following formation control using onboard sensor information. *IEEE Transactions on Robotics*, 24(6):1457–1462, Dec 2008.

[17] M. Egerstedt and X. Hu. Formation constrained multi-agent control. *IEEE Transactions on Robotics and Automation*, 17(6):947–951, Dec 2001.

[18] J. Baillieul and A. Suri. Information patterns and hedging brocketts theorem in controlling vehicle formations. In *IEEE International Conference on Decision and Control*, pages 556–563, Dec 2003.

[19] T. H. A. van den Broek, N. van de Wouw, and H. Nijmeijer. Formation control of unicycle mobile robots: a virtual structure approach. In *48th IEEE Conference on Decision and Control*, pages 8328–8333, Dec 2009.

[20] Z. Lin, B. Francis, , and M. Maggiore. Necessary and sufficient graphical conditions for formation control of unicycles. *IEEE Transactions on Automatic Control*, 50(1):540–545, January 2005.

[21] D. V. Dimarogonas and K. J. Kyriakopoulos. A connection between formation infeasibility and velocity alignment in kinematic multi-agent systems. *Automatica*, 44(10):2648–2654, October 2008.